
**Molecular Crystals and Liquid Crystals**
Publication details, including instructions for authors and subscription information:
http://www.informaworld.com/smpp/title~content=t713644168

# Low-Temperature and Wide Ferroelectric Phase in Mixtures of Chiral and Non-Chiral Tilted Smectic C-Type Liquid Crystals

Chien-Tung Liao[a]; Zheng-Long Wu[a]; Nien-Chieh Wu[a]; Jung-Yo Liu[a]; Ming-Hui Jiang[a]; Sing-Fang Zou[a]; Jiunn-Yih Lee[a]
[a] Department of Polymer Engineering, National Taiwan University of Science and Technology, Taipei, Taiwan, R.O.C.

First published on: 14 December 2010

**To cite this Article** Liao, Chien-Tung , Wu, Zheng-Long , Wu, Nien-Chieh , Liu, Jung-Yo , Jiang, Ming-Hui , Zou, Sing-Fang and Lee, Jiunn-Yih(2010) 'Low-Temperature and Wide Ferroelectric Phase in Mixtures of Chiral and Non-Chiral Tilted Smectic C-Type Liquid Crystals', Molecular Crystals and Liquid Crystals, 533: 1, 3 — 15
**To link to this Article: DOI:** 10.1080/15421406.2010.504507
**URL:** http://dx.doi.org/10.1080/15421406.2010.504507

*Mol. Cryst. Liq. Cryst.*, Vol. 533: pp. 3–15, 2010

ISSN: 1542-1406 print/1563-5287 online
DOI: 10.1080/15421406.2010.504507

Taylor & Francis
Taylor & Francis Group

# Low-Temperature and Wide Ferroelectric Phase in Mixtures of Chiral and Non-Chiral Tilted Smectic C-Type Liquid Crystals

CHIEN-TUNG LIAO, ZHENG-LONG WU, NIEN-CHIEH WU, JUNG-YO LIU, MING-HUI JIANG, SING-FANG ZOU, AND JIUNN-YIH LEE

Department of Polymer Engineering, National Taiwan University of Science and Technology, Taipei, Taiwan, R.O.C.

*A new liquid crystal of siloxane dimer with an achiral swallow-tail,* ***C11Si3C11****, was synthesized and mixed with a chiral material of 4′-(1-butoxy-1-oxopropan-2-yloxy)biphenyl-4-yl 3-bromo-4-[9-(1,1,2,2,3,3,3-hepta-methyltrisiloxanyl)nonyloxy) benzoate,* ***C9SiFLC****, for the preparation of binary mixtures for the study. The mesophases under discussion were investigated by means of polarizing microscopy (POM), differential scanning calorimetry (DSC), X-ray diffraction (XRD), and electro-optical experiments. The influence of the mixture proportion of* ***C9SiFLC*** *on the occurrence of the chiral smectic C (SmC*) phase was investigated. Finally, the electro-optical properties of the SmC* phase, such as the tilt angle and switching behavior, were also measured.*

**Keywords** Achiral siloxane dimer; chiral swallow-tail; electro-optical properties; switching behavior



## Introduction

Two interesting aspects of amphiphilic molecules such as siloxane-terminated smectogens are the reduced degree of out-of-layer fluctuations and the added control of core–core correlation in the smectic layer that is afforded by siloxane nanosegregation. In the mesophases the siloxane group microseparates and forms what could be regarded as an effective polymer backbone [1–3]. This molecular arrangement confers on the materials some of the robust mechanical properties of polymers but retains the fast electro-optic response of the low-molar-mass liquid-crystal moiety. Due to their potential for applications, low-molar-mass organosiloxane liquid crystals are presently the object of intense investigations [4–8]. However, it has been shown that binary mixtures of an achiral swallow-tailed compound [9] with an antiferro-electric liquid-crystal (S)-MHPOBC display V-shaped switching of the electro-optical response in antiferroelectric liquid-crystal mixtures. Moreover, the

Address correspondence to Jiunn-Yih Lee, Department of Polymer Engineering, National Taiwan University of Science and Technology, Taipei, Taiwan, R.O.C. E-mail: jlee@mail.ntust.edu.tw

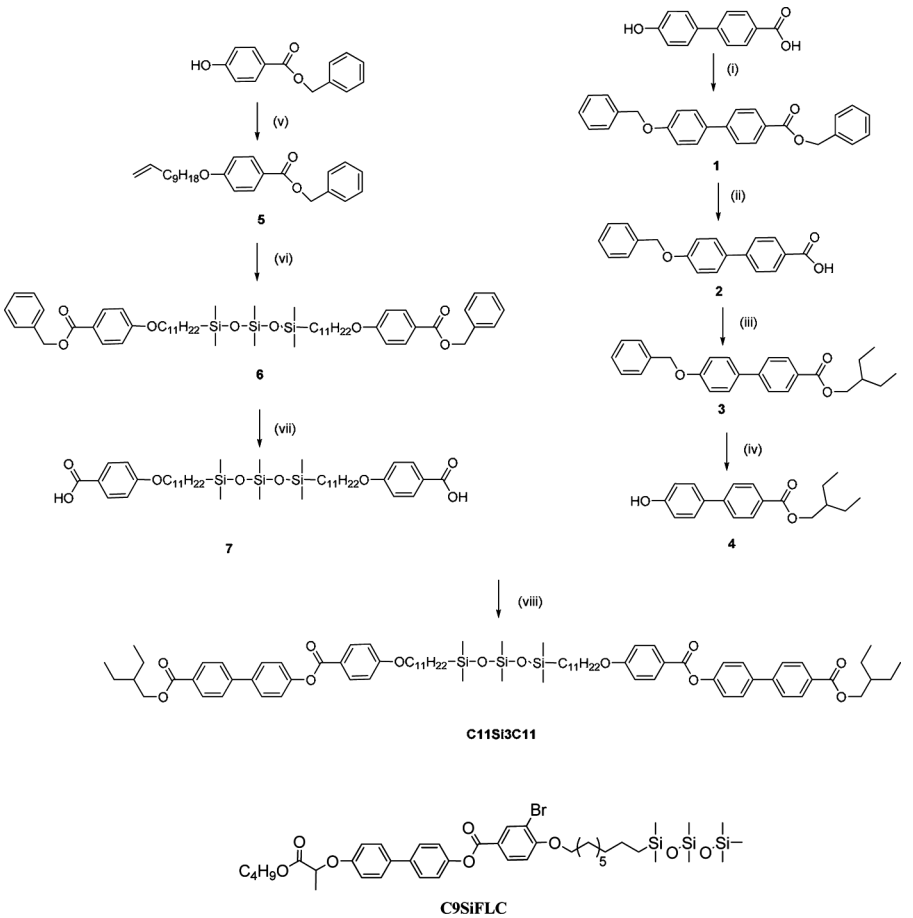


**Scheme 1.** Synthetic routes of intermediates and the target molecule.

V-shaped switching appears at a relatively high amount of achiral swallowed-tailed compound, suggesting that this optical switching can take place at a relatively low polarization [10]. This present article is a study of the ferroelectric and antiferroelectric phases in the monomesogenic (AB-type) and the bimesogenic (ABA-type) materials. A more detailed description of the synthesis and properties of the materials in these series is given in separate publications [11]. In the AB molecules a single mesogen unit A is attached to the siloxy group B, and in the ABA molecules two mesogen units are attached symmetrically to the siloxy group. As a reference base to assess the effects of the siloxy group on the behavior of the materials, we also characterized the vinyl terminated mesogenic precursors in a previous submission. Controlling molecular aggregations by doping is one of the most effective methods for organizing molecules in mesophases and is also important for inducing novel and excellent properties in materials [12, 13]. In liquid-crystal smectic C (Sm*C*) phases, helical superstructures of chiral Sm*C* (Sm*C**) phases have been induced by doping with a chiral dopant [14–17]. The helicities originate in the small rotational angle of the tilt direction on passing from one layer to the next. A more effective dopant is expected to yield a larger rotational angle. Therefore, we decided to investigate an achiral

swallow-tailed dimer to induce wide temperatures of the ferroelectric phase. A new siloxane dimer with an achiral swallow-tail, **C11Si3C11, D**, was designed and synthesized for mixing with ferroelectric liquid crystal, **C9SiFLC** [18], **F**, whose structure is shown in Scheme 1, for the preparation of ferroelectric liquid-crystal (FLC) mixtures. We examined the influence of the addition of siloxane dimer, **C11Si3C11**, on the phase transition. Finally, the properties of the smectic $C^*$ phase, such as the spontaneous polarization as a function of temperature and tilt angle, were measured for mixtures.

## Experimental

$^1$H NMR spectra were recorded on a Bruker Avance-500 spectrometer (500 MHz), using $CDCl_3$ as the solvent. Elemental analyses for C and H were performed on a Heraeus VarioEL-III elemental analyzer. The optical textures of mesophases were characterized by polarizing optical microscopy (POM; Olympus BH5) equipped with a hot stage (Mettler Toledo FP82HT) and a programmable temperature controller (Mettler Toledo FP90 central processor). Temperatures and enthalpies of transitions were determined by differential scanning calorimetry (DSC; Perkin Elmer Diamond, Taiwan). Powder samples of ca. 3.0 mg were examined at heating and cooling rates of $5^\circ C\,min^{-1}$ under a nitrogen atmosphere.

Synchrotron powder X-ray diffraction (XRD) measurements were performed in transmission geometry with synchrotron radiation at beamline BL17A of the National Synchrotron Radiation Research Center (NSRRC), Taiwan, where the X-ray wavelength was 1.33366 Å. The XRD data were collected using a Mar345 image plate detector mounted orthogonal to the beam with a sample-to-detector distance of 280 mm. The diffraction signals were accumulated for 10 sec. The powder samples were packed into a capillary tube and heated by a heat gun, for which the temperature controller was programmable by a PC with a proportional integral derivative (PID) feedback system. The scattering angle theta was calibrated by a mixture of silver behenate and silicon.

Electro-optical investigations were carried out using commercially available liquid crystal cells with indium tin oxide (ITO) electrodes coated with antiparallel rubbed polyimide (from Mesostate Corp., Taiwan, cell gap = 7.5 μm for active area = 1 $cm^2$). The sample was filled into the cell in the isotropic phase. A digital oscilloscope (Yokogawa Elect., DL1640) was used in these measurements, and a high-power amplifier was connected to an arbitrary function generator (Tektronix AWG2005, Taiwan). The switching polarization experiment was measured using a triangular waveform voltage method under slow cooling from the isotropic phase. A digital oscilloscope was used in these measurements, a high-power amplifier was connected to a function generator, and a dc power supply was utilized in the dc field experiments. During the electro-optical measurements, the modulations of textures with the application of electric fields were observed using a polarizing optical microscope.

### *Materials*

All reagents and chemicals were purchased from commercial sources (Alfa, TCI, and Fluka) and were used as received without further purification. Tetrahydrofuran (THF) and dichloromethane ($CH_2Cl_2$, DCM) were distilled to stay anhydrous before use. Reactions were monitored by thin-layer chromatography (TLC) on silica gel plates (Merck TLC silica gel 60 $F_{254}$ aluminum sheets), which were examined under

ultraviolet (UV) light and iodine vapor. Column chromatography was performed using a Merck 60-mesh silica gel. The percentages of all components for the binary mixtures were mentioned as weight ratios. We prepared the binary mixtures by mixing with DCM solvent, and the mixtures were stirred about 6–7 days until solvent evaporated.

### *Synthesis*

The general synthetic routes of the intermediates and target molecule are shown in Scheme 1. The purity and chemical structures of the intermediates and target compounds can be easily verified by TLC, $^1$H NMR spectroscopy, and elemental analysis. The synthetic procedures and chemical analyses of each product are described sequentially below.

*Benzyl 4′-(benzyloxy)biphenyl-4-carboxylate,* ***1***. This compound was prepared according to published procedures [19] as a white solid at 86% yield. $^1$H NMR (ppm, $CDCl_3$): 5.12 (s, 2H), 5.38 (s, 2H), 7.08 (d, $J = 9.0$ Hz, 2H), 7.24–7.48 (m, 10H), 7.58 (d, $J = 8.7$ Hz, 2H), 7.63 (d, $J = 8.7$ Hz, 2H), 8.13 (d, $J = 8.7$ Hz, 2H); HRMS (ESI), $m/z$, 394.6222; Anal. Calc. for $C_{27}H_{22}O_3$: C, 82.21; H, 5.62; Found: C, 82.53; H, 5.53.

*4′-(Benzyloxy)biphenyl-4-carboxylic acid,* ***2***. This compound was prepared according to published procedures [19] as a white solid at 90% yield. $^1$H NMR (ppm, $CDCl_3$): 5.13 (s, 2H), 7.05 (d, $J = 8.7$ Hz, 2H), 7.22–7.45 (m, 5H), 7.53 (d, $J = 8.7$ Hz, 2H), 7.63 (d, $J = 8.7$ Hz, 2H), 8.12 (d, $J = 8.7$ Hz, 2H); HRMS (ESI), $m/z$, 304.2922; Anal. Calc. for $C_{20}H_{16}O_3$: C, 78.93; H, 5.30; Found: C, 78.87; H, 5.39.

*2-Ethylbutyl 4′-(benzyloxy)biphenyl-4-carboxylate,* ***3***. To a suspension of compounds **2** (9.09 g, 29.9 mmol) and 2-ethylbutan-1-ol (1.39 g, 13.6 mmol), dissolved in dry dichloromethane (100 mL), *N,N*-dicyclohexylcarbodiimide (DCC, 6.2 g, 29.9 mmol) and 4-(*N,N*-dimethylamino) pyridine (DMAP, 0.33 g, 2.72 mmol) were added to react under nitrogen. The reaction mixture was stirred for 12 h at room temperature. The precipitated dicyclohexylurea (DCU) was filtered off and washed with an excess of dichloromethane (50 mL). The filtrate was washed with water and dried over anhydrous magnesium sulfate. After removal of the solvent by evaporation under reduced pressure, the residue was purified by column chromatography on silica gel using chloroform as an eluent. The collected product was crystallized from a mixture of dichloromethane and 2-propanol to give **3** as a white solid at 85% yield. $^1$H NMR (ppm, $CDCl_3$): 0.96 (t, $J = 7.5$ Hz, 6H), 1.43–1.62 (m, 4H), 1.93 (m, 1H), 4.28 (d, $J = 5.7$ Hz, 2H), 5.13 (s, 2H), 7.09 (d, $J = 8.7$ Hz, 2H), 7.32–7.47 (m, 5H), 7.58 (d, $J = 8.7$ Hz, 2H), 7.63 (d, $J = 8.4$ Hz, 2H), 8.09 (d, $J = 8.4$ Hz, 2H); HRMS (ESI), $m/z$, 388.2613; Anal. Calc. for $C_{26}H_{28}O_3$: C, 80.38; H, 7.26; Found: C, 80.32; H, 7.33.

*2-Ethylbutyl 4′-hydroxybiphenyl-4-carboxylate,* ***4***. This compound was prepared according to published procedures [19] as a white solid at 92% yield. $^1$H NMR (ppm, $CDCl_3$): 0.94 (t, $J = 7.2$ Hz, 6H), 1.45–1.60 (m, 4H), 1.64–1.70 (m, 1H), 4.28 (d, $J = 5.7$ Hz, 2H), 5.07 (s, 1H), 6.95 (d, $J = 8.7$ Hz, 2H), 7.59 (d, $J = 9.0$ Hz, 2H), 7.62 (d, $J = 8.1$ Hz, 2H), 8.09 (d, $J = 8.7$ Hz, 2H); HRMS (ESI), $m/z$, 388.2613; HRMS

(ESI), $m/z$, 298.1979; Anal. Calc. for $C_{19}H_{22}O_3$: C, 76.48; H, 7.43; Found: C, 76.29; H, 7.38.

*Benzyl 4-(undec-10-enyloxy)benzoate,* **5**. To 10.95 g (48 mmol) of benzyl 4-hydroxybenzoate, 8.16 g (48 mmol) of undec-10-en-1-ol, and 13.4 g (51 mmol) of triphenylphosphine, 150 mL of anhydrous tetrahydrofuran was introduced. To this mixture, a solution of 8.0 mL (51 mmol) of diethyl azodicarboxylate in 20 mL of anhydrous tetrahydrofuran was added dropwise. The reaction mixture was kept under argon atmosphere and stirred overnight at room temperature. After removal of the solvent by evaporation under reduced pressure, the residue was purified by column chromatography on silica gel using dichloromethane-hexane as an eluent. The collected product was crystallized from 2-propanol to give **5** as a white solid at 65% yield. $^1$H NMR (ppm, $CDCl_3$): 1.55 (m, 12H), 1.7 (m, 2H), 2.1 (m, 2H), 4.02 (m, 2H), 5.0 (m, 2H), 5.34, (s, 2H), 5.8 (m, 1H), 6.9 (d, $J = 8.7$ Hz, 2H), 7.45 (m, 5H), 8.03 (d, $J = 8.7$ Hz, 2H); HRMS (ESI), $m/z$, 380.2929; Anal. Calc. for $C_{25}H_{32}O_3$: C, 78.91; H, 8.48; Found: C, 78.77; H, 8.49.

*Siloxane dimer with benzyl benzoate moieties,* ***6***. To a degassed solution of 8.74 g (23 mmol) of compound **5** in 50 mL of anhydrous toluene, 2.6 mL (10 mmol) of 1,1,3,3,5,5-hexamethyltrisiloxane was added. The solution was stirred under argon atmosphere and 1.6 mL of a solution of dicyclopentadienylplatinum(II) chloride in anhydrous dichloromethane (2 mg mL$^{-1}$; e.g., 400 ppm per silane function) was introduced. The reaction mixture was heated up to 70°C for 24 h. Then, toluene was evaporated and the residue was purified by column chromatography on silica gel, using dichloromethane-hexane as an eluent to give 9.32 g of colorless oil at 92% yield. $^1$H NMR (ppm, $CDCl_3$): 0.05 (m, 18H), 0.52 (t, $J = 6.9$ Hz, 4H), 1.26–1.42 (m, 32H), 1.73 (m, 4H), 4.03 (t, $J = 6.9$ Hz, 4H), 5.34 (s, 4H), 7.47 (m, 10H), 6.93 (d, $J = 8.7$ Hz, 4H), 8.02 (d, $J = 8.7$ Hz, 4H); HRMS (ESI), $m/z$, 968.5391; Anal. Calc. for $C_{56}H_{84}O_8Si_3$: C, 69.37; H, 8.73; Found: C, 69.28; H, 8.69.

*Siloxane dimer with benzoic acid moieties,* ***7***. A suspension of 450 mg of 5% palladium on activated carbon in 20 mL of anhydrous tetrahydrofuran was charged with a solution of 3.56 g (3.68 mmol) of benzyl benzoate-based siloxane dimer **6** in 15 mL of anhydrous tetrahydrofuran. Hydrogen gas was allowed to slightly bubble into the reaction mixture at room temperature. The reaction was run to completion as followed by thin-layer chromatography. The mixture was filtered through Celite and then through a 0.45-mm pore-sized filter. The filtrate was finally concentrated and dried out without further purification to give 2.47 g of white crystals at 95% yield. $^1$H NMR (ppm, $CDCl_3$): 0.05 (m, 18H), 0.55 (t, $J = 6.9$ Hz, 4H), 1.23–1.42 (m, 32H), 1.7 (m, 4H), 4.04 (t, $J = 6.9$ Hz, 4H), 6.92 (d, $J = 8.7$ Hz, 4H), 8.02 (d, $J = 8.7$ Hz, 4H); HRMS (ESI), $m/z$, 788.4512; Anal. Calc. for $C_{42}H_{72}O_8Si_3$: C, 63.91; H, 9.19; Found: C, 63.89; H, 9.15.

*Siloxane dimer with mesogenic moieties,* ***C11Si3C11***. The target compound was prepared using a similar method as that described for compound **3**. After the workup, the crude products were purified by column chromatography on silica gel using dichloromethane-hexane as an eluent and twice recrystallized from 2-propanol, producing a white liquid crystal. The yields of these products after purification were ca. 62%. $^1$H NMR (ppm, $CDCl_3$): 0.02–0.06 (m, 18H), 0.52 (t, $J = 6.9$ Hz, 4H), 0.97 (t, $J = 7.5$ Hz, 12H), 1.29–1.69 (m, 40H), 1.71–1.78 (m, 2H),

1.80–1.87 (m, 4H), 4.05 (t, $J = 6.6$ Hz, 4H), 4.29 (d, $J = 6.0$ Hz, 4H), 6.99 (d, $J = 8.7$ Hz, 4H), 7.31 (d, $J = 9.0$ Hz, 4H), 7.67 (d, $J = 8.7$ Hz, 4H), 8.12 (d, $J = 8.4$ Hz, 4H), 8.17 (d, $J = 8.7$ Hz, 4H); HRMS (ESI), $m/z$, 1349.7555; Anal. Calc. for $C_{80}H_{112}O_{12}Si_3$: C, 71.17; H, 8.36; Found: C, 71.22; H, 8.29.

*4′-(1-Butoxy-1-oxopropan-2-yloxy)biphenyl-4-yl 3-bromo- 4-[9-(1,1,2,2,3,3,3-heptamethyltrisiloxanyl)nonyloxy) benzoate,* ***C9SiFLC****.* Yield 86%, as a white liquid crystal,[1]H NMR (ppm, $CDCl_3$): 0.01(s, 21H), 0.08–0.10 (m, 2H), 0.89 (t, $J = 7.5$ Hz, 3H), 1.26–1.89 (m, 20H), 2.17 (m, 2H), 4.11–4.19 (m, 4H), 4.81 (m, 1H), 6.95 (m, 3H), 7.25 (d, $J = 9.0$ Hz, 2H), 7.50 (d, $J = 8.5$ Hz, 2H), 7.57 (d, $J = 8.7$ Hz, 2H), 8.12 (d, $J = 8.7$ Hz, 1H), 8.40 (s, 1H); HRMS (ESI), $m/z$, 860.3033; Anal. Calc. for $C_{42}H_{63}BrO_8Si_3$: C, 58.65; H, 7.38; Found: C, 58.59; H, 7.32.

## Results and Discussion

### *Thermal Properties and Optical Textures*

The phase behaviors of the target compound **C11Si3C11** were investigated by a combination of POM and DSC. The phase transition temperatures observed by POM match well with the corresponding DSC thermograms. The mesomorphic properties of the studied compound **C11Si3C11**, the phase sequence, and the phase transition temperatures are summarized in Table 1. Upon cooling from the isotropic state, the compound **C11Si3C11** displays a characteristic broken fan texture of the mesophase at 132°C (see Fig. 1a), indicating the formation of the SmC phase. The compound **C9SiFLC** displays a characteristic Schlieren texture and broken fan texture of the mesophase at 40°C (see Fig. 1b), indicating the formation of the SmC* phase; the texture that appears below the isotropic state of the 20% **C9SiFLC**–80% **C11Si3C11** (**20F /80D**) mixture is uniform, with a characteristic Schlieren texture and broken fan texture of the mesophase at 110°C (see Fig. 1c), indicating the formation of the SmC* phase. The other mixtures show similar optical textures as the mixture **20F/80D**, thereby implying that they have the same mesophase. All of the mixtures exhibit enantiotropic mesomorphic behavior and only a mesophase. Based on comparisons between the compound **C9SiFLC** and the **20F/80D** mixture upon cooling from the isotropic liquid, the mixture is owing to the lower clearing transition temperature than before and forms only a mesophase. The result shows

**Table 1.** Phase Transition Temperatures (°C) for the Mixtures as Determined by DSC with First Cooling (Scan Rate = 5°C $min^{-1}$)[a]

| Mixture | I | | SmC | | SmC* | | Cr |
|---|---|---|---|---|---|---|---|
| 100F/0D | • | | | 59.5 | • | <−20 | • |
| 80F/20D | • | | | 69.6 | • | <−20 | • |
| 60F/40D | • | | | 100.2 | • | <−20 | • |
| 40F/60D | • | | | 113.5 | • | <−20 | • |
| 20F/80D | • | | | 130.2 | • | <−20 | • |
| 0F/100D | • | 154.1 | • | | | −9.3 | • |

[a]Cr = crystalline phase; SmC = smectic C phase; SmC* = chiral SmC phase; I = isotropic phase, • = phase exists; F = **C9SiFLC**; D = **C11Si3C11**.

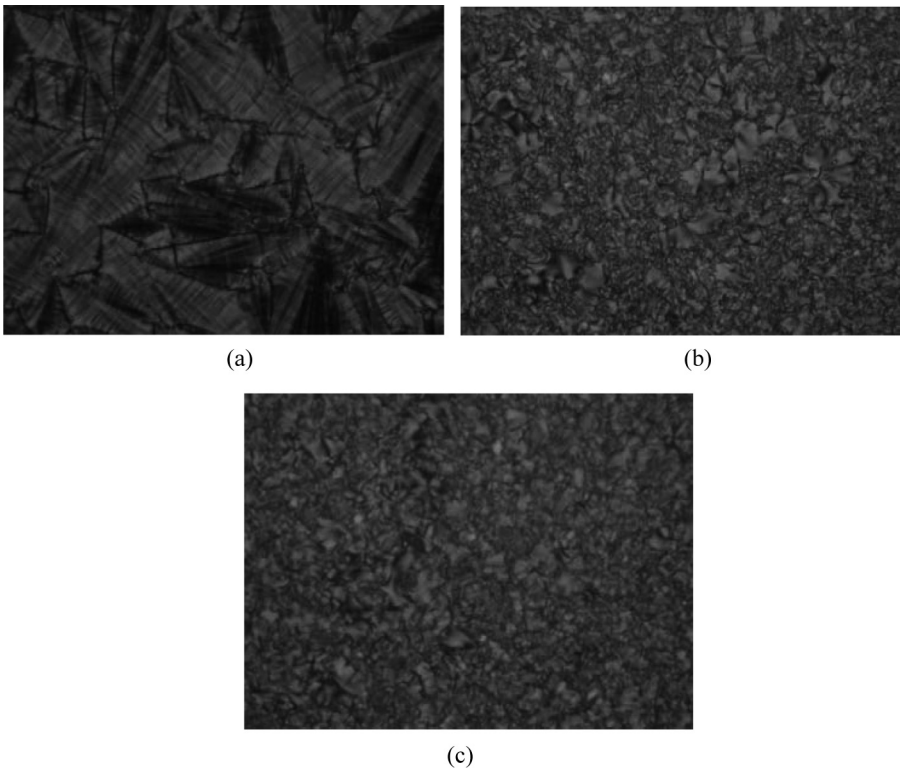




**Figure 1.** Polarized optical microscopic textures include (a) broken fan texture in SmC phase at 132°C on cooling (1°C/min) from the isotropic state for compound **C11Si3C11**; Schlieren texture and broken fan texture in SmC* phase (b) at 40°C for compound **C9SiFLC**, and (c) at 110°C for the mixture 20% **C9SiFLC**–80% **C11Si3C11** (**20F/80D**).

that when a small amount of the chiral dopant molecules (**C9SiFLC)** is added to the compound **C11Si3C11**, it weakens the interlayer. Generally, the **C9SiFLC** molecule is also considered to be a chiral dopant unit, but due to its size and flexibility it disrupts the interlayer interface and weakens the layers. As a result, when the mixture has more **C9SiFLC** molecules, the clearing temperature of the mixture is decreased. Thus, size and flexibility effects of the **C9SiFLC** molecules have profound influences on their mesomorphic behavior. In contrast, when the dimer **C11Si3C11** is added to the compound **C9SiFLC**, the SmC* phase temperature range increases with the increase in the proportion.

### *XRD Studies*

To further identify the type of mesophases and determine the structural parameters, further investigations were performed using XRD. As shown in Fig. 2a, the 2D diffraction pattern on the meridian XRD pattern of the mixture **20F/80D** is integrated, as an illustrated example. The resulting XRD pattern of the mixture **20F/80D** at 50°C exhibits three Bragg reflections in the small-angle region at $2\theta = 2.14$, 4.28, and 6.42, with *d*-spacings of 35.7, 17.9, and 11.9, respectively, corresponding to

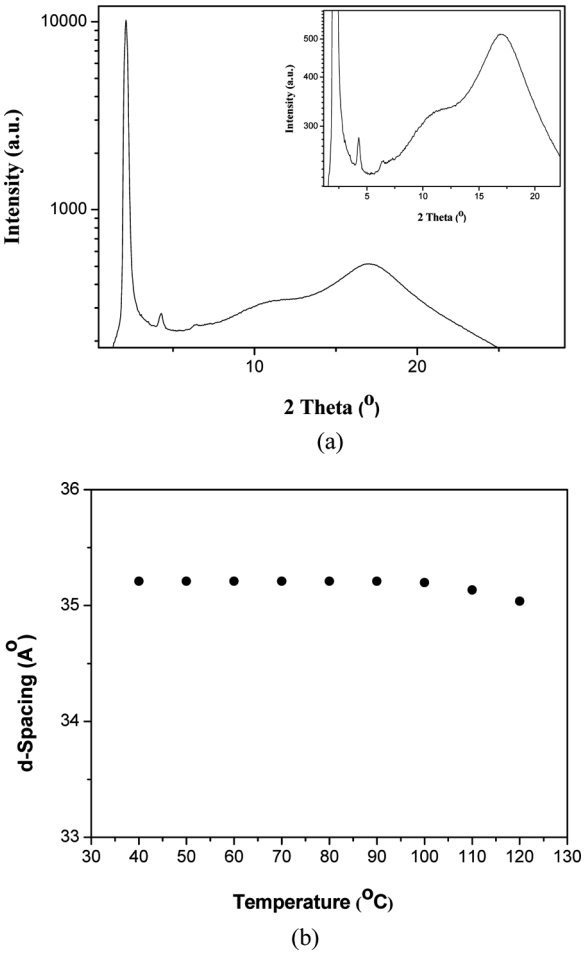




**Figure 2.** (a) X-ray diffraction intensity against angle profile obtained in the SmC* phase of mixture **20F/80D** at 50°C (upon cooling from the isotropic phase) and (b) layer *d*-spacing as a function of the temperature dependence.

the reciprocal spacing in the rations 1, 2, and 3 to the indexation $(hk) = (10)$, (20), and (30), which can imply the formation of a layered structure. On the other hand, a diffuse scattering halo in the wide-angle region centered at $2\theta$ around 17.0° with a *d*-spacing of ca. 4.5 Å indicates a liquid-like arrangement of the molecules within the layers. As shown in Fig. 2b, the temperature dependence of the layer *d*-spacing of the mixture **20F/80D** was recorded upon cooling from the isotropic phase. The values of the layer *d*-spacing were observed to only slightly change within the temperature range of the mesophase. Mixtures also revealed similar diffraction patterns at temperatures within the respective mesophase temperature ranges. Therefore, the fact that the layer *d*-spacing value of 35.9 Å for compound **C9SiFLC** by XRD measurement is smaller than the calculated theoretical molecular length of 48.2 Å suggests a tilted arrangement of smectic structure; that is, smectic C phase with a tilt angle of 25.3° along the layer normal direction. As a result, when the mixture has more **C11Si3C11** molecules, the layer *d*-spacing of the mixture is similar. It seems that

the tilt angle of compound **C9SiFLC** is not influenced by the increase in the proportion of the dimer **C11Si3C11** molecule. The interpretation of the small-angle X-ray scattering (SAXS) measurements (see Fig. 2a) display on the double halo at wide angle (evidence of siloxane-paraffinic nanosegregation), and acknowledge the fact that these compounds are known to form intercalated bilayer structures, which might explain why the d-spacing of **C9SiFLC** does not change much upon addition of the dimer **C11Si3C11**.

### *Electro-Optical Behavior*

The switching behavior was observed in the SmC* phase of the studied mixture **60 F/40D** using the triangular wave method. One distinct sharp peak per half period of an applied triangular wave voltage is clearly seen under a triangular wave field of about 150 Vpp at 60 Hz (see Fig. 3a). This is a strong indication of a ferroelectric switching process. To clarify this, we also measured the polarization by the Diamant-Bridge method [20] (see Fig. 3b) and observed only a single hysteresis loop down to the lowest frequency (1 Hz) available in the measurement, again indicating ferroelectric-type switching. The temperature dependence of the magnitude of the *P*s value for the



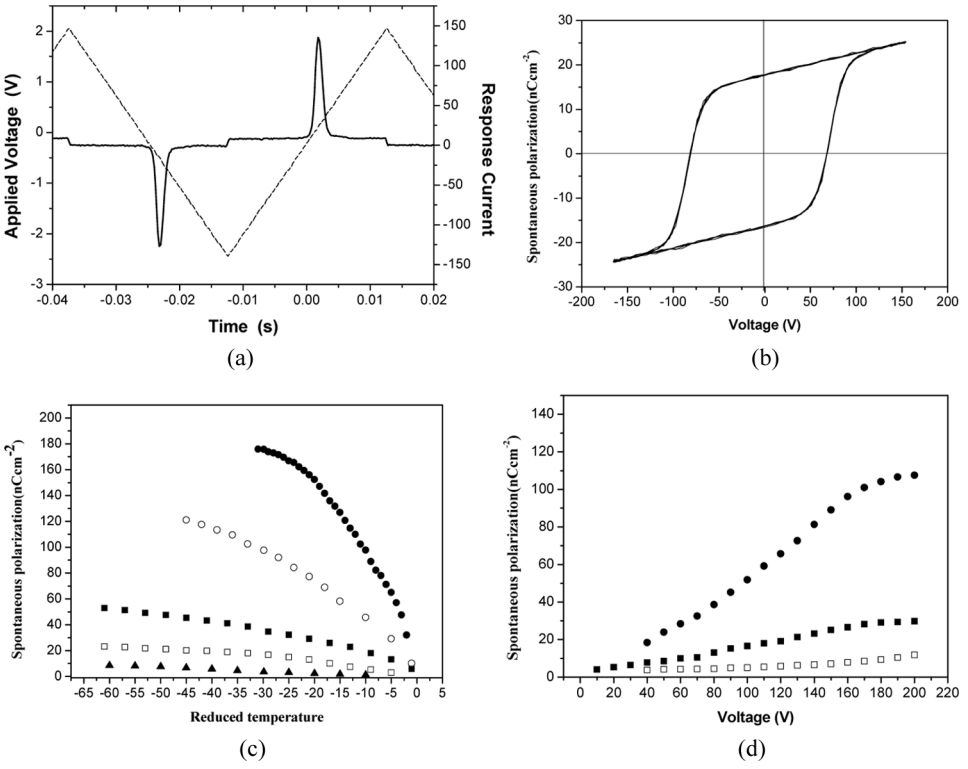


**Figure 3.** (a) Switching current response observed in the SmC* phase of the mixture **60F/40D** at 90°C under the applied triangular wave voltage (7.5 μm antiparallel rubbed polyimide-coated ITO cell, 150 Vpp, 60 Hz) and (b) bridge method. Summary of spontaneous polarization (*P*s) as a function of the (c) temperature and (d) voltage (Tc – T = 10°C) observed in the SmC* phase of mixtures. The reduced temperature means T (measured temperature)– Tc (clearing point). ●: **100F/0D**: ○: **80F/20D**: ■: **60F/40D**: □: **40F/60D**: ▲: **20F/80D**.

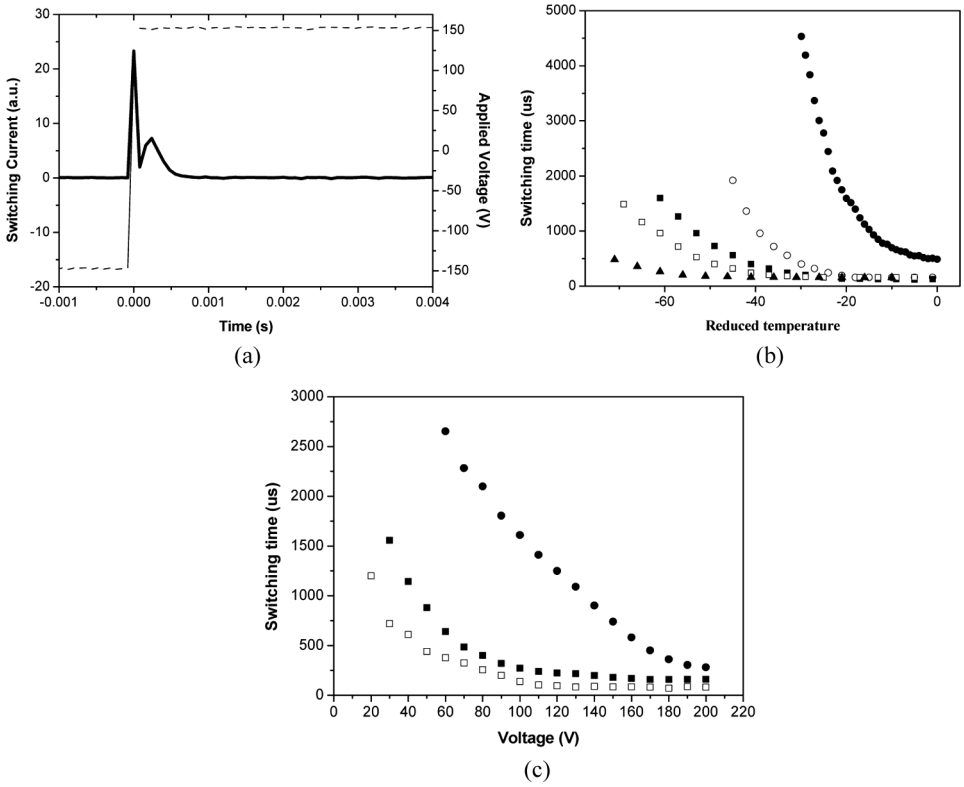


**Figure 4.** (a) The time dependences of the switching current under a square wave field for the mixture **80F/20D** at 45°C. The switching time as a function of (b) temperature and (c) voltage for target mixtures (on antiparallel rubbing direction LC cells with 7.5-μm thickness as Vpp = 150 V, f = 10 Hz). The reduced temperature means T (measured temperature)− Tc (clearing point). ●: **100F/0D**: ○: **80F/20D**: ■: **60F/40D**: □: **40F/60D**: ▲: **20F/80D**.



mixtures obtained by integrating the area under the one peak is shown in Fig. 3c. It can be seen that the *P*s is dependent on the temperature of the mixtures. The abrupt increase of *P*s around the isotropization temperature indicates that the phase transformation from the isotropic phase to the SmC* phase is a first-order phase transformation. It is also observed that the value of Ps increases with decrease in temperature for the compounds. The increase in the Ps value with decrease in the temperature may be due to the strong P-E (polarization–electric field) coupling and P-$\theta$ (polarization-tilt angle) coupling [21]. We also see the behavior of spontaneous polarization with applied voltage, which is shown in Fig. 3d. Because the molecular helical order in the sample may not be suppressed completely by the confining substrates, it was observed that with an increase in the applied voltage, the spontaneous polarization increases sharply initially. However, the applied field may also induce a transition to higher order phase, which does not exist in the phase diagram without an applied field. We find an increment in the polarization value with increasing voltage. In liquid-crystal smectic C (Sm*C*) phases of the dimer **C11Si3C11, D**, helical superstructures of chiral Sm*C* (Sm*C**) phases were induced

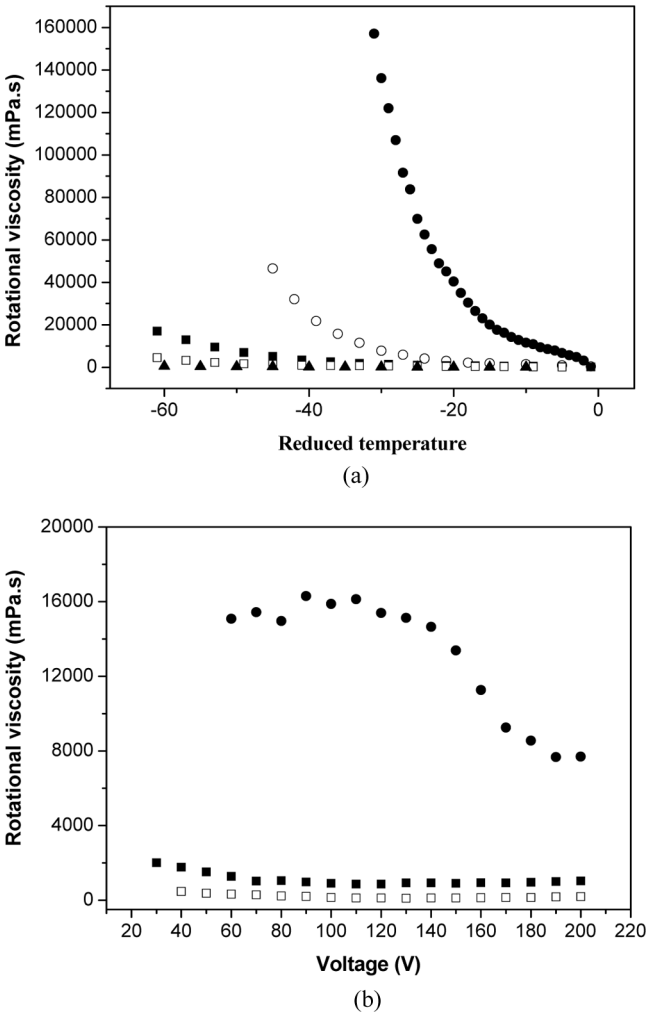




**Figure 5.** Behavior of rotational viscosity for target compounds with different (a) temperature and (b) voltage. The reduced temperature means T (measured temperature)− Tc (clearing point). ●: **100F/0D**: ○: **80F/20D**: ■: **60F/40D**: □: **40F/60D**: ▲: **20F/80D**.

by doping with the chiral material **C9SiFLC, F**. As a result, it seems that the maximum Ps value increases as the amount of chiral material **F** increases.

To investigate the dynamics of the polarization switching behavior, the switching currents of the mixture **80F/20D** were measured with an applied square wave field (as Vpp = 150 V, f = 10 Hz) in the SmC* phase. The switching current curves of the mixture **80F/20D** at 45°C are shown in Fig. 4a as a function of time. The switching time ($\tau$) values are determined from the time elapsed between the appearance of the maximum of the current signal and the field reversal [22]. The switching time as a function of the temperature is shown in Fig. 4b with the same field and frequency (i.e., Vpp = 150 V, f = 10 Hz). The decrease of the switching time with increasing temperature for mixtures is observed due to the viscosity decrease. The switching time with applied voltage is shown in Fig. 4c. The switching time decreases

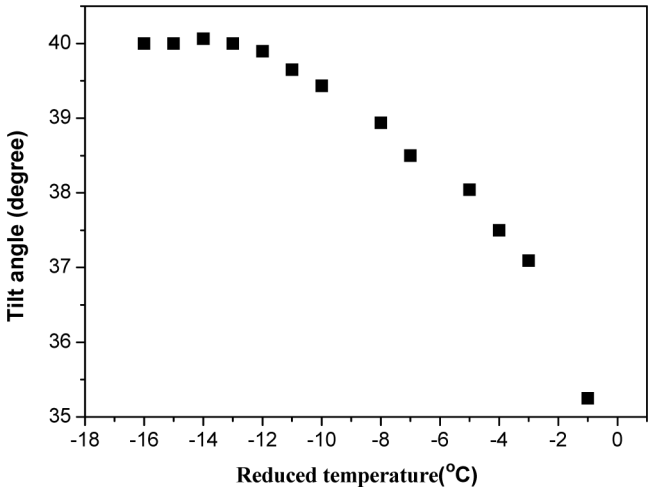


**Figure 6.** Tilt angle of the SmC* phase as a function of the dc electric fields in the mixture **80F/20D** (on antiparallel rubbing direction LC cells with 7.5 μm thickness). The reduced temperature means T (measured temperature)– Tc (clearing point).



with increasing voltage. We see the behavior of spontaneous polarization; we find an increment in the polarization value for mixtures.

The combined effect of the switching time and the spontaneous polarization can be seen in the behavior of rotational viscosity. The behavior of rotational viscosity for mixtures with different temperatures and voltages can be seen in Fig. 5a and Fig. 5b. These three are related to each other by the following relation:

$$\gamma_\psi = \tau P_s E \tag{1}$$

where $\tau$ is switching time, $\gamma_\psi$ is the rotational viscosity, *Ps* is the spontaneous polarization, and $E$ is the applied field. The rotational viscosity decreases, the spontaneous polarization increases, and the switching time decreases in accordance with Eq. (1). As seen in the results, it seems that the mixtures have smaller *Ps* values than pure **C9SiFLC, F**, but their switching times are smaller due to the smaller viscosity with the increase in the proportion of the **C11Si3C11** molecule, **D**.

The measured optical tilt angle as a function of temperature for the SmC* phase for the mixture **80F/20D** is shown in Fig. 6. In general, the optical tilt angles increase with decreasing temperature and exhibit maxima. The maximum optical angle for the mixture **80F/20D** is about 40°. Mixtures also revealed similar tilt angles at around 40° at temperatures within the respective mesophase temperature range of X-ray diffraction (XRD) measurements.

## Conclusions

We have achieved the molecular design, synthesis, and characterization of a liquid crystal that has-siloxane dimer with an achiral swallow-tail, **C11Si3C11**. Specifically, we have explored the possibility of stabilizing a wide thermal range chiral smectic C (SmC*) phase in the mixture with the ferroelectric liquid crystal, **C9SiFLC**.

It exhibits the SmC* phase over a 150°C thermal range in the mixture **80F/20C**. Electro-optic studies were carried out for the majority of the mixtures exhibiting the SmC* phase. Electrical switching and molecular tilt angle were investigated in the SmC* phase.

## Acknowledgment

We thank Dr. Jey-Jau Lee for help with the XRD experiments at the National Synchrotron Radiation Research Center (NSRRC, for the beamline BL17A) in Taiwan. Financial support from the National Science Council of Taiwan (ROC) through 98-2221-E-011-004 is gratefully acknowledged.

## References

[1] Coles, H. J., Owen, H., Newton, J., & Hodge, P. (1993). *Liq. Cryst.*, *15*, 739.
[2] Newton, J., Coles, H. J., Owen, H., & Hodge, P. (1993). *Ferroelectrics*, *148*, 379.
[3] Wischerhoff, E., & Zentel, R. (1995). *Liq. Cryst.*, *18*, 745.
[4] Robinson, W. K., Kloess, P. S., Carboni, C., & Coles, H. J. (1997). *Liq. Cryst.*, *23*, 309.
[5] Naciri, J., Ruth, J., Crawford, G., Shashidar, R., & Ratna, B. R. (1995). *Chem. Mater.*, *7*, 1397.
[6] Maksimova, G. V., Matveev, L. G., Kopylov, V. M., & Obedkova, N. N. (1995). *Vysokomolekulyarnye Soedineniya A & B*, *37*, 558.
[7] Saez, I. M., Styring, P., Paterson, N., & Sinn, E. (1997). *Abstract of Papers of Am. Chem. Soc.*, *214*, 91.
[8] Ibn-elhaj, M., Skoulios, A., Guillon, D., Newton, J., Hodge, P., & Coles, H. J. (1995). *Liq. Cryst.*, *19*, 373.
[9] Wu, S. L., & Chiang, C. T. (2002). *Liq. Cryst.*, *29*, 39.
[10] Wu, S. L., & Lin, C. Y. (2003). *Liq. Cryst.*, *30*, 205.
[11] Kloess, P. S., McComb, J., & Coles, H. J. (1996). *Ferroelectrics*, *180*, 233.
[12] Gregg, B. A., & Cormier, R. A. (2001). *J. Am. Chem. Soc.*, *123*, 7959.
[13] Thisayukta, J., Niwano, H., Takezoe, H., & Watanabe, J. (2002). *J. Am. Chem. Soc.*, *124*, 3354.
[14] Sasaki, T., Katsuragi, A., & Ohno, K. (2002). *J. Phys. Chem. B*, *106*, 2520.
[15] Thisayukta, J., Nakayama, Y., Kawachi, S., Takezoe, H., & Watanabe, J. (2000). *J. Am. Chem. Soc.*, *122*, 7441.
[16] Maly, K. E., Wand, M. D., & Lemieux, R. P. (2002). *J. Am. Chem. Soc.*, *124*, 7898.
[17] Vizitiu, D., Lazar, C., Halden, B. J., & Lemieux, R. P. (1999). *J. Am. Chem. Soc.*, *121*, 8229.
[18] Liao, C. T., Lee, J. Y., & Lai, C. C. (2010). *Mater. Chem. Phys.* (accepted).
[19] Michael, V. P., William, K., Wilfrid, A. K., & Richard, A. I. D. (1990). *J. Chem. Soc. Perkin Trans.*, *9*, 2501.
[20] Diamant, H., Drenck, K., & Pepinsky, R. (1957). *Rev. Sci. Instrum.*, *28*, 30.
[21] Raina, K. K., & Kumar, P. (2009). *Indian Inst. Sci.*, *89*(2), 243.
[22] Yelamaggad, C. V., Hiremath, U. S., Anitha Nagamani, S., Shankar Rao, D. S., & Krishna Prasad, S. (2001). *J. Mater. Chem.*, *2*, 1818.